

RECENT RESULTS FROM MARK II AT SPEAR AND PEP*

J. Strait
(Representing the Mark II Collaboration)¹⁾
Stanford Linear Accelerator Center
Stanford University, Stanford, California 94305

and

Lawrence Berkeley Laboratory and Department of Physics
University of California, Berkeley, California 94720

ABSTRACT

Three results are presented: (1) The semi-leptonic branching ratio of the Λ_c has been measured at SPEAR to be $B(\Lambda_c^+ \rightarrow e^+X) = (4.5 \pm 1.7)\%$. (2) Properties of τ -pair production have been measured at PEP at $\sqrt{S} = 29$ GeV: $\sigma^{\tau\tau}/\sigma^{\text{QED}} = 0.97 \pm 0.05 \pm 0.06$; the forward-backward asymmetry is $A_{\tau\tau} = (-3.5 \pm 5.0)\%$; inclusive branching ratios are $B(\tau \rightarrow 1 \text{ Prong}) = (86 \pm 4)\%$, $B(\tau \rightarrow 3 \text{ Prongs}) = (14 \pm 4)\%$, $B(\tau \rightarrow 5 \text{ Prongs}) < 0.6\%$ (95% C.L.). (3) A search has been performed for the pair production of charged, point-like, spin 0 particles. The existence of such particles can be ruled out at a 90% confidence level for $3 \lesssim M \lesssim 10$ GeV/c² and branching ratio into hadrons $\lesssim 90\%$.

(Presented at the XVIIth Rencontre de Moriond: Electroweak Interactions and Grand Unified Theories, Les Arcs, France, March 14-20, 1982.)

* Work supported in part by the Department of Energy, contracts DE-AC03-76SF00515 and W-7405-ENG-48.

INTRODUCTION

The results of three studies by the Mark II collaboration¹⁾ are presented. First, from our continuing analysis of SPEAR data, is a measurement²⁾ of the semi-leptonic branching ratio of the charmed baryon Λ_c . Second is a study³⁾ of the characteristics of τ -pair production at PEP. Third is the search⁴⁾ for charged, point-like, spin 0 particles. The Mark II detector has been described elsewhere⁵⁾ and will not be discussed here.

SEMI-LEPTONIC BRANCHING RATIO OF THE Λ_c

The production of the Λ_c charmed baryon in e^+e^- annihilation and its decay into several hadronic modes have been clearly established.⁶⁾ We report here evidence for the observation of Λ_c semi-leptonic decay. This evidence is based on measurements of direct electron production in baryon events at center-of-mass energies above and below the threshold for charmed baryon pair production. The data sample was taken at center-of-mass energies from 4.5 to 6.8 GeV and represents an integrated luminosity of 13700 nb^{-1} . Data taken at lower energies (primarily at the $\psi'(3685)$), representing an integrated luminosity of 4300 nb^{-1} , are used to verify the absence of baryon associated direct electrons below the Λ_c threshold. Two separate baryon event samples are used -- events containing an antiproton and events containing a Λ or $\bar{\Lambda}$. Events containing a proton and not an antiproton are excluded to reduce the background from beam-gas interactions. The p and \bar{p} are identified by time-of-flight (TOF), with a somewhat looser cut for those baryons which are Λ or $\bar{\Lambda}$ decay products. The background of pions and kaons misidentified as baryons is estimated to be less than 5%. The Λ ($\bar{\Lambda}$) are identified from reconstruction of their $p\pi^-$ ($\bar{p}\pi^+$) decay modes. Background under the Λ peak due to beam-gas protons is reduced to the 20% level with a cut ($Q \leq 0$) on the total charge of those Λ events which do not contain an identified \bar{p} . The background under the $\bar{\Lambda}$ peak is very small. The overall \bar{p} and Λ , $\bar{\Lambda}$ detection efficiencies are 60% and 15% (including the $p\pi$ branching ratio) respectively.

Electrons are identified by TOF in the momentum range 100-300 MeV/c, by TOF and shower characteristics in the lead-liquid argon (LA) electromagnetic calorimeter in the range 300-500 MeV/c, and by LA alone in the range 500-1200 MeV/c. The electron selection criteria are chosen to give clean electron identification, with as little contamination by misidentified pions as possible, at the expense of a relatively low electron detection efficiency. This efficiency is deduced in two independent ways: (1) from a sample of real electrons arising from photon pair conversion, and (2) from a sample of Monte Carlo generated electron showers.

The results are in reasonable agreement. The measured efficiency as a function of momentum is shown in Fig. 1. The fractional uncertainty in the electron detection efficiency is estimated to be less than 5%.

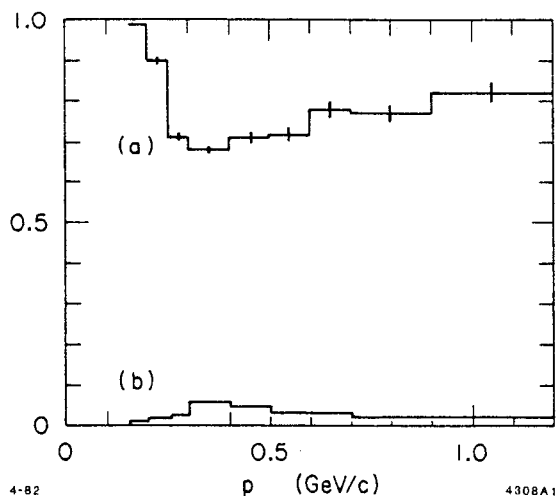


Fig. 1. Electron identification efficiency (a) and pion misidentification probability (b) for particles entering the fiducial volume of the LA shower counters.

The major background is the misidentification of charged pions as electrons. Samples of real pions, taken from reconstructed ψ and ψ' events ($\psi' \rightarrow \psi\pi^+\pi^-$ and $\psi \rightarrow 2(\pi^+\pi^-)\pi^0$ or $3(\pi^+\pi^-)\pi^0$), are used to determine the momentum dependent probabilities of misidentifying π^\pm as electrons. These probabilities, shown in Fig. 1, are used to calculate the number of misidentified pions included in the electron sample. Uncertainties in the pion misidentification probabilities are estimated at 7% overall, based on the statistics of the samples of known pions from which they are determined.

The only other significant background arises from electron-positron pairs, produced either by photon conversions in the material between the beam and the drift chamber or by Dalitz decays of π^0 's. Most e^+e^- pairs are removed either by an invariant mass cut or by a visual scan if one of the electrons was detected but not tracked by the drift chamber. A statistical subtraction is necessary to correct for the remaining e^+e^- pairs in which one electron is completely undetected. The number of electrons from this source was calculated by Monte Carlo, with the π^0 population taken as half of the π^\pm population at each momentum. Unidentified e^+e^- pairs are the dominant background at very low electron momenta, but are a negligible background above 300 MeV/c.

The results of the search for direct electrons below and above the Λ_c threshold are shown in Table I. The raw e^\pm count excludes those electrons from recognized γ conversions and π^0 Dalitz decays. The backgrounds from misidentified pions and from unidentified electron pairs are listed separately. Below Λ_c threshold, the electron rate in baryon events is consistent with zero, while above threshold, independent signals are present at the 2.6σ level in both the \bar{p} and the $\Lambda, \bar{\Lambda}$ samples. The probability of obtaining such signals if there is actually no direct electron contribution is less than 10^{-4} .

We attribute the baryon-electron events to charmed baryon pair production and subsequent semi-leptonic decay. Charmed baryon-charmed meson associated production is assumed to be negligible.⁷⁾ Events with misidentified baryons in

TABLE I. Direct electron signal in baryon events.

	$E_{c.m.} < 4.5 \text{ GeV}$		$E_{c.m.} > 4.5 \text{ GeV}$	
	9992 \bar{p}	1499 $\Lambda, \bar{\Lambda}$	5209 \bar{p}	757 $\Lambda, \bar{\Lambda}$
raw e^\pm	613 ± 25	58 ± 8	440 ± 21	73 ± 9
π^\pm bgnd	424 ± 22	51 ± 3	287 ± 14	39 ± 2
e^\pm bgnd	144 ± 16	19 ± 2	84 ± 8	12 ± 1
net e^\pm	45 ± 37	$- 12 \pm 8$	69 ± 26	22 ± 9
corrected e^\pm	105 ± 86	$- 32 \pm 23$	170 ± 64	52 ± 21

which the electrons actually arise from charmed meson semi-leptonic decay contribute at most 10% of the observed signal in the \bar{p} events, and much less in the $\Lambda, \bar{\Lambda}$ events.

We estimate the charmed baryon content of the proton and lambda samples from previous measurements of inclusive p and Λ production, $R(p)$ and $R(\Lambda)$, as functions of energy,⁸⁾ which show clear steps near the charmed baryon threshold. The fraction of p or Λ events due to charmed baryon production is taken as the increase in $R(p)$ or $R(\Lambda)$ relative to the base value of $R(p)$ or $R(\Lambda)$ below the charmed baryon threshold. Averaged over the center-of-mass energy distributions of the baryon data samples, the resulting fractions are $\Delta R(p)/R(p) = 0.45 \pm 0.07$ and $\Delta R(\Lambda)/R(\Lambda) = 0.57 \pm 0.14$. The fraction of charmed baryon decays leading to a proton (rather than a neutron) in the final state is taken to be $F(p) = 0.6 \pm 0.1$.⁹⁾ The fraction of charmed baryon decays leading to a lambda in the final state is then $F(\Lambda) = [\Delta R(\Lambda)/\Delta R(p)]F(p) = 0.17 \pm 0.06$. The above numbers are based on the assumption that the observed increases in $R(p)$ and $R(\Lambda)$ above the charmed baryon threshold are due entirely to charmed baryon production. If part of the increases are unassociated with charm, the true branching ratios will be correspondingly larger than those calculated below.

Since charmed baryons emit positrons, the inclusive branching ratio $BR(\Lambda_c^+ \rightarrow eX)$ can be obtained from baryon-electron and antibaryon-positron events, with the observed baryon serving only as a tag for a charmed baryon event. Semi-inclusive branching ratios $BR(\Lambda_c^+ \rightarrow peX)$ and $BR(\Lambda_c^+ \rightarrow \Lambda^0 eX)$ can be obtained from baryon-positron and antibaryon-electron events.

The resultant semi-leptonic branching ratios of the charmed baryon are $BR(\Lambda_c^+ \rightarrow e^+X) = (4.2 \pm 2.0)\%$ from the $\bar{p}-e^+$ sample and $BR(\Lambda_c^+ \rightarrow e^+X) = (5.5 \pm 3.5)\%$ from the $\bar{\Lambda}-e^+, \Lambda-e^-$ sample. Averaging these two results gives:

$$BR(\Lambda_c^+ \rightarrow e^+X) = (4.5 \pm 1.7)\% .$$

The semi-inclusive branching ratios are:

$$\text{BR}(\Lambda_c^+ \rightarrow p e^+ X) = (1.8 \pm 0.9)\%$$

and

$$\text{BR}(\Lambda_c^+ \rightarrow \Lambda^0 e^+ X) = (1.1 \pm 0.8)\% .$$

Protons from Λ^0 decay are included in $\text{BR}(\Lambda_c \rightarrow p e X)$, and lambdas from Σ^0 decay are included in $\text{BR}(\Lambda_c \rightarrow \Lambda^0 e X)$. The Cabibbo favored semi-leptonic charm decay has the isospin selection rule $|\Delta I| = 0$, and hence the hadronic decay products are expected to have isospin 0. The simplest way in which this might occur, namely through the mode $\Lambda^0 e^+ \nu$, does not seem to be dominant.

The inclusive semi-leptonic branching ratio of the Λ_c can be combined with the measured Λ_c lifetime to determine the Λ_c semi-leptonic decay rate. Using the world average lifetime¹⁰⁾ $\tau(\Lambda_c) = (2.9^{+1.3}_{-0.8}) \times 10^{-13}$ sec, we obtain $\Gamma(\Lambda_c \rightarrow e X) = (1.6 \pm 0.8) \times 10^{11}$ sec⁻¹, in good agreement with a theoretical calculation of $\Gamma(\Lambda_c \rightarrow e X) = (1.9 \pm 0.5) \times 10^{11}$ sec⁻¹.¹¹⁾

PRODUCTION OF τ -PAIRS AT PEP

The τ -pair studies and the elementary scalar search were performed with the Mark II detector operating at PEP at a center-of-mass energy of 29 GeV. The data correspond to an integrated luminosity of 14.4 pb⁻¹. In the reaction $e^+e^- \rightarrow \tau^+\tau^-$, collinear τ 's are produced with the energy of the beam and decay with low multiplicity. Thus τ production gives events with two low mass, low multiplicity, back-to-back jets. To reduce systematic errors due to uncertainties in branching fractions, events are selected on the basis of these topological characteristics, and dependence on specific decay modes is avoided.

The particles in each event are divided into two groups by the plane perpendicular to the thrust axis and the following requirements are made:

- (1) 1 to 3 charged particles in each group,
- (2) total energy (charged + neutral) $\geq E_{c.m.}/4$,
- (3) each group has an invariant mass $< 2 \text{ GeV}/c^2$,
- (4) all the charged particles in at least one group have momentum $< 8 \text{ GeV}/c$,
- (5) the highest momentum particle in at least one of the groups has momentum above 2 GeV/c, enters the liquid argon fiducial volume, and deposits an energy less than 30% of its momentum,
- (6) both groups cannot contain exactly one particle that is a muon with momentum above 2 GeV/c,
- (7) for the highest momentum particle in each group, the TOF is within 3 ns of the expected time,

(8) the difference in total charge between the two groups is not zero, and
 (9) the acollinearity angle between the two groups is $< 50^\circ$.
 Criteria (1) and (3) reject hadronic events; criterion (2) rejects two photon events; criterion (4) rejects μ -pair events; criterion (5) rejects Bhabha events; criterion (6) rejects $e^+e^- \rightarrow e^+e^-\mu^+\mu^-$ and μ -pair events; and criterion (7) rejects cosmic rays. Criterion (8) is necessary to determine which group of particles came from the τ^+ . Criterion (9) prevents higher order QED corrections from being too large.

There are 470 τ -pair events satisfying the above criteria. Several corrections are applied to these data. From Bhabha events, it is determined that (1) the TOF system is $98.0 \pm 0.2\%$ efficient (the inefficiency is primarily due to cracks between the counters), (2) the charged particle trigger is $98.6 \pm 0.2\%$ efficient, and (3) the total energy trigger is $98.4 \pm 0.2\%$ efficient.

A Monte Carlo program is used to determine the detector response to τ -pair events and to possible backgrounds. Raw data generated by the Monte Carlo is processed by the same tracking, vertexing, and filtering routines used for the actual data. The simulation of the detector includes electromagnetic and hadronic interactions in the material surrounding the interaction region. For the efficiency calculation and comparison of the data with QED, a Monte Carlo event generator¹²⁾ of order α^3 is used.

The backgrounds in the τ -pair sample are given in Table II; sources not listed have been calculated to be negligible. The backgrounds are determined from Monte Carlo simulations, but have been verified with the data where possible. The calculation of the μ -pair and $e^+e^-\mu^+\mu^-$ backgrounds is confirmed by a rise in the 2 prong acoplanarity¹³⁾ distribution at very small angles ($< 1^\circ$). Events with the invariant mass of one group of particles between 2 and 3 GeV/c^2 confirm the hadronic background. The other backgrounds in Table II are small and reliably calculated.

TABLE II. Background contributions to τ -pair events.

Background Source	Fraction of Signal (%)
$e^+e^- \rightarrow e^+e^-$	0.3 ± 0.3
$\rightarrow \mu^+\mu^-$	1.6 ± 0.2
\rightarrow hadrons	4.3 ± 1.3
$\rightarrow e^+e^-\mu^+\mu^-$	6.1 ± 0.6
$\rightarrow e^+e^-\tau^+\tau^-$	0.9 ± 0.1

To study the multiplicity distribution from τ decays, the selection criteria were relaxed to allow up to 5 charged particles from each τ . The background subtracted multiplicity distribution (Fig. 2) shows that the τ decays primarily to 1 or 3 charged particles. Without background subtraction, there are 6 τ candidates with 5 charged particles; however, 7.6 ± 0.6 are expected from γ conversions in 1 and 3 prong τ decays. This yields an upper limit of $B(\tau \rightarrow 5 \text{ prongs}) < 0.6\%$ (95% C.L.).

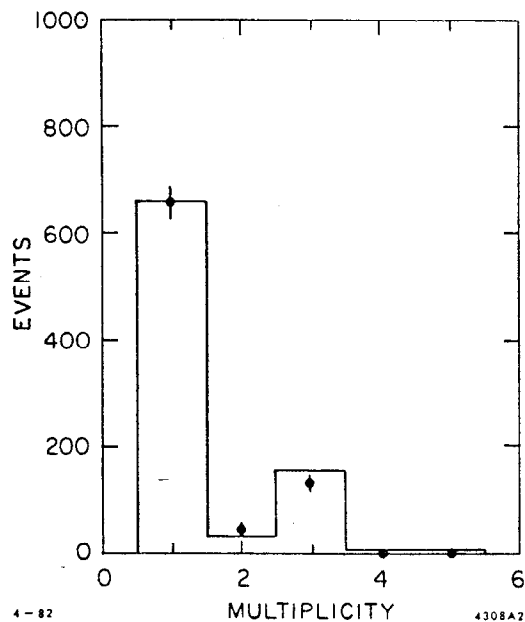


Fig. 2. Observed τ decay multiplicity distribution. The solid histogram is the result of an unfold fit.

of $B(\tau \rightarrow \pi^- \pi^+ \pi^- \eta \pi^0) = 18 \pm 7\%$.

Sources of systematic error on the normalization are summarized in Table III. The error due to uncertainties in τ branching fractions is determined from the efficiency of individual decay modes and the errors on their measured rates.^{17),18)} Tau-pair events are lost due to interaction of pions in the liquid argon shower counters, since tight cuts are used to eliminate Bhabha events. The Monte Carlo simulates pion interactions using energy deposition distributions obtained from a clean, hand-selected sample of $\tau \rightarrow 3\pi\nu_\tau$ decays. Varying the predicted 60% pion identification efficiency from 50% to 70% changes the τ -pair efficiency by $\pm 2.4\%$. The α^3 QED calculation is checked by comparing the observed and predicted acollinearity distributions (Fig. 3). The contribution of α^4 QED terms to the τ -pair cross section has been estimated in Table III simply by squaring the α^3 correction.

To account properly for γ conversions and particle detection efficiencies in determining the produced τ decay multiplicity distribution, an unfold method¹⁴⁾ was used. Only the 1, 2 and 3 prong decays were included in the fit, which gives $B(\tau \rightarrow 1 \text{ prong}) = 86 \pm 4 \pm 1\%$ and $B(\tau \rightarrow 3 \text{ prongs}) = 14 \pm 4 \pm 1\%$. The systematic error is due to uncertainties in the background multiplicity distribution. This value of $B(\tau \rightarrow 1 \text{ prong})$ is higher than either the world average¹⁵⁾ of $68 \pm 10\%$ or a recent TASSO measurement¹⁶⁾ of $76 \pm 6\%$. The discrepancy might be due to earlier experiments not correcting for γ conversions as the unfold method properly does. The 3 prong inclusive branching fraction is consistent with a Mark I measurement¹⁷⁾

Table III

Systematic errors in τ -pair normalization.

Source	Error (%)
Luminosity	3.0
τ Branching fractions	2.8
Interacting π 's	2.4
Higher order QED	1.9
Backgrounds	1.7
Monte Carlo Statistics	0.8
Total	5.5

In contrast to the normalization, the angular asymmetry has very small uncertainties. Only detector biases which are both charge and polar angle dependent can cause systematic changes in the asymmetry. The trigger and

detection efficiencies and the momentum resolution have been measured with Bhabha events and are independent of the particle charge and polar angle within the central region of the detector. The dominant errors in the asymmetry measurement come from Monte Carlo statistics and possible α^4 QED contributions. The asymmetry expected¹²⁾ from QED is +0.3% within the Mark II acceptance.

The total cross section normalized to the small angle luminosity monitor³⁾ agrees well with the predictions of QED:

$$\sigma^{\tau\tau}/\sigma^{\text{QED}} = 0.97 \pm 0.05 \pm 0.05 .$$

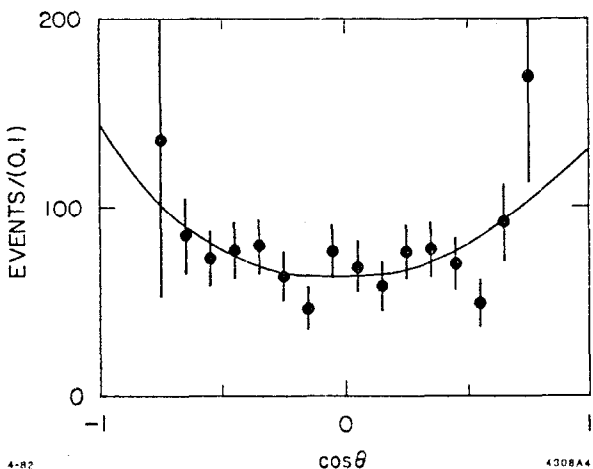


Fig. 4. Angular distributions for τ -pair events. The curve is the prediction of QED to order α^3 .

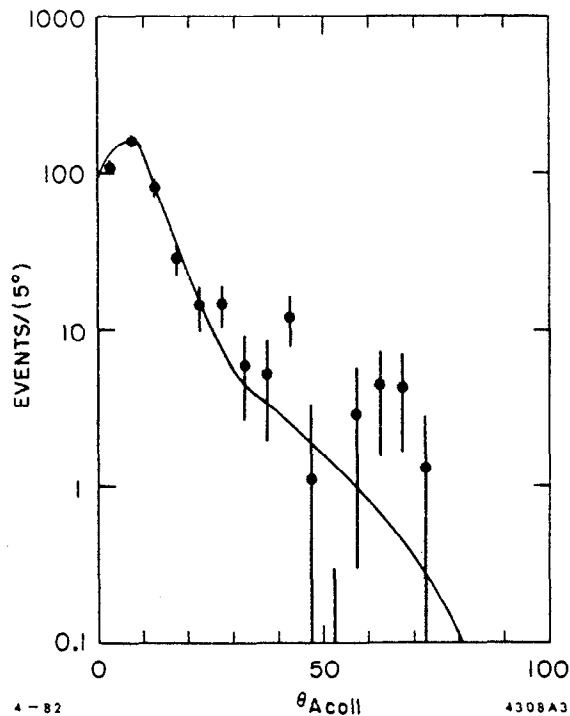


Fig. 3. Acollinearity angle distribution for τ -pair events. The curve is the prediction of QED to order α^3 .

The τ -pair angular distribution is shown in Fig. 4. The polar angle θ is defined to be the angle between the thrust axis, taken in the direction of the more positive group of particles, and the positron beam direction. Monte Carlo studies show that the thrust axis reproduces the τ direction within $\sim 5^\circ$. The τ -pair angular distribution, Fig. 4, shows good agreement with the predictions of QED.

To lowest order in all coupling constants, the τ -pair production cross

section is:¹⁹⁾

$$\frac{d\sigma}{d\Omega} = \frac{\alpha^2}{4s} [F_1(1 + \cos^2\theta) + F_2\cos\theta]$$

$$F_1 = 1 + Rg_v^2$$

$$F_2 = 2Rg_a^2$$

$$R = \frac{\sqrt{2}G_F}{2\pi\alpha} \frac{m_Z^2}{(s - m_Z^2)} s ,$$

where θ is the polar scattering angle, g_v and g_a are the vector and axial-vector neutral current couplings, G_F is the Fermi coupling, m_Z is the mass of the Z^0 , and s is the square of the center-of-mass energy. R was calculated in the limit $m_Z \rightarrow \infty$, which underestimates g^2 by $\sim 10\%$ if $m_Z = 90$ GeV. In general, g_v and g_a can be different for the electron, muon, and tau. Allowing for this, each g^2 is actually $g^e g^\tau$.

The weak neutral current couplings have been determined by doing a maximum likelihood fit of the absolutely normalized angular distribution to predictions of α^3 QED modified by weak effects. For the normalization, the systematic errors in Table III are included as an additional term in the likelihood function. The results of the fit are:

$$g_a^\tau g_a^e = 0.19 \pm 0.29$$

$$g_v^\tau g_v^e = 0.16 \pm 0.26 .$$

The error on g_v^2 has roughly equal statistical and systematic components. These results are in agreement with the expectations of the standard model²⁰⁾ which predicts $g_a^2 = 0.25$ and $g_v^2 = 0.002$ for $\sin^2\theta_w = 0.23 \pm 0.01$.²¹⁾ However, at the present level of statistics, these values also agree with the absence of weak effects ($g_v = g_a = 0$).

SEARCH FOR ELEMENTARY (PSEUDO) SCALARS

In currently accepted gauge theories of weak interactions,²⁰⁾ fermions and gauge bosons acquire masses from spontaneous symmetry breaking. This is achieved through fundamental Higgs fields or composite scalar fields (technicolor theories.²²⁾) The standard model has only one physical, neutral Higgs boson, whose couplings to fermions are proportional to the fermion mass. Other models may have additional, charged Higgs bosons, whose couplings are not as rigidly

fixed as in the minimal model. Dynamical symmetry breaking models introduce a new strong interaction at a scale of ~ 1 TeV, which results in a rich spectrum of pseudo-Goldstone bosons²³⁾ (technipions) some of which are expected to have masses of a few GeV. No Higgs boson or technipion, charged or neutral, has yet been observed.

We have search for charged Higgs particles or technipions (hereafter referred to as a Higgs and represented by H^\pm) at PEP. Higgs pairs are assumed to be produced via the reaction

$$e^+e^- \rightarrow H^+H^-$$

with a cross section of

$$\frac{d\sigma}{d\Omega} = \frac{\alpha^2 \beta^3 \sin^2 \theta}{8s}$$

where β is the velocity of the Higgs in units of the speed of light. The Higgs is assumed to decay to the heaviest fermions possible, either heavy quarks or the heavy lepton τ . Two cases have been considered: (1) both Higgs decay to ν_τ and (2) one Higgs decays to hadrons and the other to ν_τ .

The characteristics expected from Higgs pair production are calculated from a Monte Carlo simulation program which produces a pair of Higgs according to the differential cross section given above. When a Higgs decays to a $c\bar{s}$ pair, the quarks are hadronized by a standard Feynman-Field program. The only property of the hadronic decay of the Higgs which is crucial to this analysis is the charged multiplicity distribution. The average charged multiplicity of a Higgs decay in the Monte Carlo agrees with e^+e^- results at an equivalent energy. The rest of the analysis is based on the kinematics of producing particle pairs and not on the details of quark fragmentation into hadrons. If the Higgs decays to ν_τ , the τ is allowed to decay according to the measured branching ratios.

To search for events in which both Higgs decay to ν_τ , the previously selected τ -pair events are examined for extra missing transverse momentum from the Higgs decay. In the plane perpendicular to the beam, the axis is chosen relative to which the transverse momentum is equal for the two groups of particles. This common transverse momentum is given by

$$P_T = \frac{|(\vec{p}_1 \times \vec{p}_2) \cdot \hat{z}|}{|(\vec{p}_1 \cdot \vec{p}_2) \times \hat{z}|},$$

where \hat{z} is the unit vector in the beam direction. The observed P_T distribution (Fig. 5) is well fit by the τ -pair Monte Carlo and no evidence for Higgs-pair production is seen. The data are fit to a sum of the τ -pair Monte Carlo and the Higgs Monte Carlo for various masses of the Higgs with the branching ratio of the Higgs into τ 's as the only free parameter. The 90% C.L. limits are shown by

curve I of Fig. 6; the left boundary of curve I is at the τ mass. The existence of a charge Higgs with mass less than m_τ and couplings proportional to mass is excluded by the measured properties of the τ , such as the equality of the muonic and electronic decay rates.

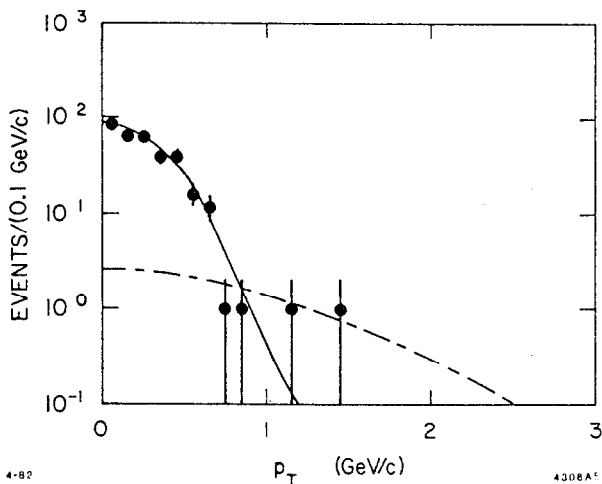


Fig. 5. P_T distribution for τ -pair events. The solid curve is the expectation for τ -pair production. The dashed curve is the expectation for a Higgs with mass $7 \text{ GeV}/c^2$ and $B(H \rightarrow \tau\nu_\tau) = 1$.

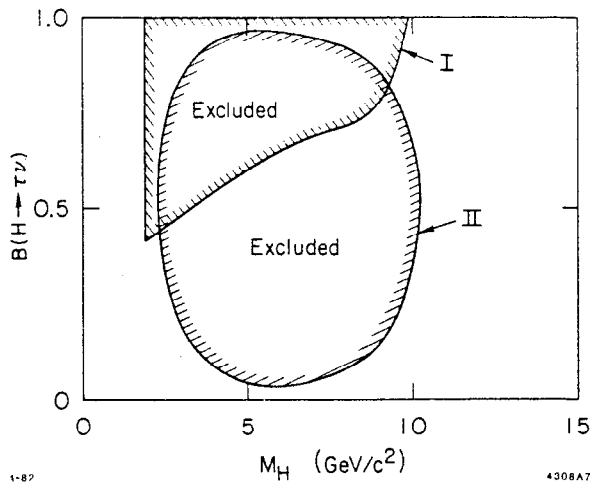


Fig. 6. Excluded regions (90% C.L.) for events in which both Higgs decays to $\tau\nu_\tau$ (curve I) or one Higgs decays to hadrons and the other to $\tau\nu_\tau$ (curve II).

To look for events in which one Higgs decays to hadrons and the other to $\tau\nu_\tau$, events with one charged particle (from the τ) opposite a multiprong jet are selected. The particles in each event are divided into two groups by the plane perpendicular to the thrust axis the following criteria applied:

- (1) $E_{\text{tot}} > \sqrt{s}/4$ (charged + neutral energy),
- (2) one group of particles has exactly one charged track, less than three photons, and an invariant mass $< 2 \text{ GeV}/c^2$,
- (3) the other group of particles has at least three charged particles, any number of photons, and invariant mass greater than $2 \text{ GeV}/c^2$, and
- (4) events are rejected if the most energetic particle in both groups is an electron.

Criterion (1) rejects two photon events, and criterion (4) rejects radiative Bhabha events with a gamma conversion in the material surrounding the interaction region.

The P_T distribution for the 22 events meeting the above criteria is shown in Fig. 7. All of the events fall at low P_T , typical of normal hadronic events. The solid curve is the prediction of a Monte Carlo for hadronic production normalized by a factor of 0.5 to agree with the observed number of events. The

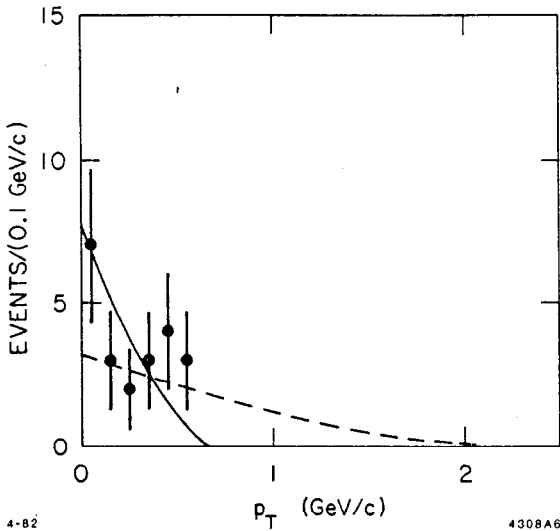


Fig. 7. P_T distribution for events with 1 prong opposite a multi-prong jet. The solid curve is the prediction of the hadron Monte Carlo normalized to the data. The dashed curve is the expectation for a Higgs with mass $7 \text{ GeV}/c^2$ and $B(H \rightarrow \text{hadrons}) = B(H \rightarrow \tau\nu_\tau) = 0.5$.

dashed curve shows the expected P_T distribution for a Higgs with mass $7 \text{ GeV}/c^2$ and $B(H \rightarrow \text{hadrons}) = B(H \rightarrow \tau\nu_\tau) = 0.5$. The discrimination between Higgs production and the background is at large P_T . A cut of $P_T = 0.6 \text{ GeV}/c$ is chosen solely from the Monte Carlo curves to maximize the statistical significance of a potential Higgs signal for a mass of $7 \text{ GeV}/c^2$ and $B(H \rightarrow \text{hadrons}) = B(H \rightarrow \tau\nu_\tau) = 0.5$. Assuming that the Higgs decays only to hadrons or to $\tau\nu_\tau$, the absence of events above $P_T = 0.6 \text{ GeV}/c$ leads to limits (90% C.L.) on branching fractions as a function of mass as shown by curve II of Fig. 6. The left boundary is due to the P_T spectrum from Higgs decay narrowing as the mass is reduced. The

right boundary is due to the β^3 threshold term in the production cross section.

The shape of the excluded region in Fig. 2 is relatively insensitive to the P_T cut. Increasing the cut to $0.7 \text{ GeV}/c$ moves the left boundary of the excluded region from $\sim 3 \text{ GeV}/c^2$ to $\sim 4 \text{ GeV}/c^2$ and changes the rest of the contour very little. Decreasing the P_T cut to $0.5 \text{ GeV}/c$ has a larger effect due to the 3 events between 0.5 and $0.6 \text{ GeV}/c$; the excluded region extends from $M_H = \sim 3.5$ to $\sim 8 \text{ GeV}/c^2$ and from $B_T = \sim 10$ to $\sim 90\%$. The shape of the excluded region in Fig. 6 is insensitive to whether the Higgs decays to $c\bar{s}$, $c\bar{b}$, or $u\bar{d}$ in the Monte Carlo.

Combining the two cases we can exclude any charged, point-like, spin 0 particles coupling primarily to heavy fermions and having a mass less than $\sim 10 \text{ GeV}/c^2$ and a branching fraction to hadron less than $\sim 90\%$.

REFERENCES

1. G. S. Abrams, D. Amidei, A. Bäcker, C. A. Blocker, A. Blondel, A. M. Boyarski, M. Breidenbach, D. L. Burke, W. Chinowsky, G. von Dardel, W. E. Dieterle, J. B. Dillon, J. Dorenbosch, J. M. Dorfan, M. W. Eaton, G. J. Feldman, M. E. B. Franklin, G. Gidal, L. Gladney, G. Goldhaber, L. J. Golding, G. Hanson, R. J. Hollebeek, W. R. Innes, J. A. Jaros, A. D. Johnson, J. A. Kadyk, A. J. Lankford, R. R. Larsen, B. LeClaire, M. Levi, N. Lockyer, B. Löhr, V. Lüth, C. Matteuzzi, M. E. Nelson, J. F. Patrick, M. L. Perl, B. Richter, A. Roussarie, T. Schaad, H. Schellman, D. Schlatter, R. F. Schwitters, J. L. Siegrist, J. Strait, G. H. Trilling, E. Vella, R. A. Vidal, Y. Wang, J. M. Weiss, M. Werlen, J. M. Yelton, C. Zaiser, and G. Zhao; Stanford Linear Accelerator Center, Stanford University, Stanford, California 94305; Lawrence Berkeley Laboratory and Department of Physics, University of California, Berkeley, California 94720; Department of Physics, Harvard University, Cambridge, Massachusetts 02138.
2. E. Vella et al., SLAC-PUB-2898, submitted to Phys. Rev. Lett.
3. C. A. Blocker et al., to be submitted to Phys. Rev. D.
4. C. A. Blocker et al., to be submitted to Phys. Rev. Lett.
5. W. Davies-White et al., Nucl. Instrum. Methods 160, 227 (1979); G. S. Abrams et al., IEEE Trans. Nucl. Sci. NS-25, 309 (1978); G. S. Abrams et al., Phys. Rev. Lett. 43, 477 (1979).
6. G. S. Abrams et al., Phys. Rev. Lett. 44, 10 (1980).
7. M. W. Coles, Ph.D. Thesis, University of California, Berkeley, LBL-11513 (1980). An associated production rate of 20% (near the present upper limit), combined with an average D semi-leptonic branching ratio of 8%, would reduce the calculated Λ_c inclusive semi-leptonic branching ratio from 4.5% to 3.6%.
8. E. N. Vella, Ph.D. Thesis, University of California, Berkeley, LBL-13845 (1981). The values of $R(\Lambda)$ used here are 20% lower than the previously published values⁶) because the previous calculation used an incorrect Λ^0 detection efficiency.
9. This value is based on a simple isospin statistical model.
10. L. Montanet, talk at this conference.
11. N. Cabibbo and L. Maiani, Phys. Lett. 79B, 109 (1978); A. Ali and E. Pietarinen, Nucl. Phys. B154, 519 (1979); N. Cabibbo, G. Corbo and L. Maiani, Nucl. Phys. B155, 93 (1979). The semi-leptonic width and error quoted here are based on a charmed quark mass $m_c = (1.75 \pm 0.10) \text{ GeV}/c^2$.
12. F. A. Berends and R. Kleiss, Nucl. Phys. B177, 237 (1981); F. A. Berends, K. J. F. Gaemers and R. Gastmans, Nucl. Phys. B63, 381 (1973), Nucl. Phys. B68, 541 (1974); F. A. Berends and G. J. Komen, Phys. Lett. 63B, 432 (1976).
13. The acoplanarity angle is the angle between the plane containing one final state particle and the beam and the plane containing the other final state particle and the beam.
14. J. L. Siegrist et al., SLAC-PUB-2831, submitted to Phys. Rev. D.
15. Particle Data Book, Rev. of Mod. Phys. 52 (1980).
16. R. Brandelik et al., Phys. Lett. 92B, 199 (1980).
17. J. A. Jaros et al., Phys. Rev. Lett. 40, 1120 (1978).

18. C. A. Blocker et al., SLAC-PUB-2820, to be published in Phys. Lett.;
C. A. Blocker et al., SLAC-PUB-2886, submitted to Phys. Rev. Lett.;
G. S. Abrams et al., Phys. Rev. Lett. 43, 1555 (1979); J. M. Dorfan et al.,
Phys. Rev. Lett. 46, 215 (1981); G. Alexander et al., Phys. Lett. 73B, 99
(1978).
19. P. Dittman and V. Hepp, Z. f. Phys. C10, 283 (1981).
20. S. L. Glashow, Nucl. Phys. 22, 579 (1961), Rev. Mod. Phys. 52, 539 (1980);
A. Salam, Phys. Rev. 127, 331 (1962), Rev. Mod. Phys. 52, 525 (1980);
S. Weinberg, Phys. Rev. Lett. 19, 1264 (1967), Rev. Mod. Phys. 52, 515
(1980).
21. K. Winter, Proc. of the 1979 Symposium on Lepton and Photon Interactions
at High Energies, Fermilab 371 (1979); P. Langacker et al., Proc. of the
Neutrino 79, Bergen, 276 (1979).
22. L. Susskind, Phys. Rev. Lett. 19, 2619 (1979); S. Weinberg, Phys. Rev. D
13, 974 (1976).
23. S. Dimopoulos, Nucl. Phys. B168, 69 (1980).